Intermolecular interactions of thrombospondins drive their accumulation in extracellular matrix

Dae Joong Kim[a,*,†], Elena D. Christofidou[b,*,‡], Douglas R. Keene[c], Marwah Hassan Milde[a], and Josephine C. Adams[a,b,d]

[a]Department of Cell Biology, Lerner Research Institute, and [d]Department of Molecular Medicine, Cleveland Clinic Lerner College of Medicine, Cleveland Clinic, Cleveland, OH 44195; [b]School of Biochemistry, University of Bristol, Bristol BS8 1TD, United Kingdom; [c]Micro-Imaging Center, Shriners Hospital for Children, Portland, OR 97239

ABSTRACT **Thrombospondins participate in many aspects of tissue organization in adult tissue homeostasis, and their dysregulation contributes to pathological processes such as fibrosis and tumor progression. The incorporation of thrombospondins into extracellular matrix (ECM) as discrete puncta has been documented in various tissue and cell biological contexts, yet the underlying mechanisms remain poorly understood. We find that collagen fibrils are disorganized in multiple tissues of *Thbs1*$^{-/-}$ mice. In investigating how thrombospondins become retained within ECM and thereby affect ECM organization, we find that accumulation of thrombospondin-1 or thrombospondin-5 puncta within cell-derived ECM is controlled by a novel, conserved, surface-exposed site on the thrombospondin L-type lectin domain. This site acts to recruit thrombospondin molecules into ECM by intermolecular interactions in *trans*. This mechanism is fibronectin independent, can take place extracellularly, and is demonstrated to be direct in vitro. The *trans* intermolecular interactions can also be heterotypic—for example, between thrombospondin-1 and thrombospondin-5. These data identify a novel concept of concentration-dependent, intermolecular "matrix trapping" as a conserved mechanism that controls the accumulation and thereby the functionality of thrombospondins in ECM.**

Monitoring Editor
Kozo Kaibuchi
Nagoya University

Received: May 27, 2014
Revised: Apr 6, 2015
Accepted: May 12, 2015

This article was published online ahead of print in MBoC in Press (http://www.molbiolcell.org/cgi/doi/10.1091/mbc.E14-05-0996) on May 20, 2015.

*These authors contributed equally to this work.

Present addresses: †Department of Cell Biology and Physiology, University of North Carolina at Chapel Hill, Chapel Hill, NC 27599; ‡Department of Cell Physiology and Pharmacology, College of Medicine, University of Leicester, Leicester LE1 9HN, United Kingdom.

J.C.A. designed the study with D.J.K. and E.D.C. and analyzed data. D.J.K., E.D.C., and M.H.M. performed experiments, analyzed data, and prepared figures. D.R.K. conducted electron microscopy of collagen fibrils and contributed to data analysis. The manuscript was written by J.C.A. with D.J.K. and E.D.C. All authors approved the submitted version and declare that they have no commercial, financial, or other conflicts of interest.

Address correspondence to: Josephine Adams (jo.adams@bristol.ac.uk).

Abbreviations used: COMP, cartilage oligomeric matrix protein; ECM, extracellular matrix; mRFP, monomeric red fluorescent protein; PSACH, pseudoachondroplasia; TSP, thrombospondin; TSR, thrombospondin type 1 domain.

INTRODUCTION

Thrombospondins (TSPs) are multidomain, extracellular, calcium-binding glycoproteins that are conserved from sponges to humans (Bentley and Adams, 2010; Ozbek *et al*., 2010). The single TSP of *Drosophila* has vital roles in integrin-dependent extracellular matrix (ECM) organization at developing muscle/tendon attachment sites (Chanana *et al*., 2007; Subramanian *et al*., 2007). Mammals encode five TSPs in two structural subgroups, A and B. TSP1 and TSP2 in subgroup A are trimeric and are transient, low-abundance components of adult connective tissue that are elevated within the ECM in healing wounds, tumor stroma, and atherosclerotic lesions. Important roles identified from knockout mice include inhibition of angiogenesis, modulation of wound healing, oncoprotection, tissue-specific phenotypes, and increased susceptibility to experimental disease models (Adams, 2001; Adams and Lawler, 2011; Bornstein *et al*., 2004; Zhang and Lawler, 2007). In human populations, susceptibility to premature heart disease correlates with certain polymorphisms in *THBS1* or *THBS2* (Topol *et al*., 2001; Burke *et al*., 2010). In contrast, subgroup B TSPs, comprising TSP3, TSP4, and

TSP5 (also known as cartilage oligomeric matrix protein [COMP]), are pentameric proteins that are lifelong ECM constituents in cartilage, bone, tendon, and blood vessel walls (Hankenson *et al.*, 2010). TSP4 contributes to susceptibility to cardiovascular disease (Topol *et al.*, 2001; Stenina *et al.*, 2003; Frolova *et al.*, 2010), and mutations in *THBS5/COMP* are causal for pseudoachondroplasia (PSACH) and certain forms of multiple epiphyseal dysplasia (Posey *et al.*, 2008).

Some of these multiple roles are mediated by domains or motifs that are specific to individual family members. For example, inhibition of angiogenesis, binding of matrix metalloproteases, and binding of latent transforming growth factor β (TGFβ) by TSP1 and TSP2 derive from their multifunctional TSP type 1 domains (TSRs), which are specific to subgroup A TSPs. Latent TGFβ activation is mediated by a TSR motif, RFK, that is unique to TSP1 (Schultz-Cherry *et al.*, 1995; Crawford *et al.*, 1998; Bein and Simons, 2000; Jimenez *et al.*, 2000; Yang *et al.*, 2000; Bentley and Adams, 2010). In contrast, the extent to which the complex roles of TSPs in tissue organization and physiology depend on shared mechanisms remains poorly understood. Identification of such mechanism(s) at the molecular level would be an important step toward novel strategies to modulate physiological or pathological activities of TSPs across multiple tissue contexts.

TSPs exhibit complete conservation of domain architecture in their C-terminal region, which forms a single tertiary structure built from contiguous epidermal growth factor domains, thrombospondin type 3 repeats, and a C-terminal, L-type lectin domain (L-lectin domain; Kvansakul *et al.*, 2004; Carlson *et al.*, 2005; Tan *et al.*, 2009; Bentley and Adams, 2010; see also the later presentation of domain diagrams in Figures 2 and 5). Thus the C-terminal region and especially the L-lectin domain are of great interest for understanding potential fundamental shared roles of TSPs. The L-lectin domain of TSP-1 has been implicated in signaling by the transmembrane immunoglobulin superfamily member CD47 (Gao *et al.*, 1996; Isenberg *et al.*, 2006). However, CD47 is specific to amniotes and therefore cannot be the mediator of evolutionarily conserved activities of the L-lectin domain (Bentley and Adams, 2010). In contrast, activities attributed to the L-lectin domain of TSP5 include binding to various collagens and matrilin-3 (Posey and Hecht, 2008).

This laboratory identified previously that the C-terminal region of TSP1 in trimeric form is necessary and sufficient to mediate incorporation as discrete puncta into ECM (Adams *et al.*, 2008). This finding opened a major question on the mechanism of ECM incorporation of TSP1 and the potential conservation of this activity within the TSP family. Here we identify a novel process in ECM organization by which a conserved site on the L-lectin domain controls ECM accumulation of TSP puncta through the *trans* association of TSP molecules. We propose the novel concept that "matrix trapping" of secreted TSPs according to their local concentration is a central mechanism by which TSPs can flexibly associate with and affect the interstitial ECM of multiple tissues.

RESULTS

The absence of TSP1 affects connective ECM organization in vivo

To address whether the absence of TSP1 has biological consequences for ECM organization, we examined by electron microscopy the connective ECM of tail tendons and dermis in healthy, sex- and age-matched wild-type or *Thbs1*$^{-/-}$ mice. Tail tendons of wild-type mice contained, as expected, highly organized bundles of parallel collagen fibrils. In contrast, the fibrils of *Thbs1*$^{-/-}$ mice were of variable widths and irregularly packed, with blending, splaying, and even splitting of fibrils (Figure 1A). In cross section, the collagen fibrils of *Thbs1*$^{-/-}$ mice were irregular in profile and included fibrils that appeared larger than those of control mice, with apparent merging of adjacent fibrils (Figure 1A, overview; higher magnification in Figure 1B). Similar enlargement and disorder of collagen fibrils was apparent in the dermal ECM of *Thbs1*$^{-/-}$ mice (Figure 1A; higher magnification in Figure 1B). The images presented compare 6.5-wk-old male mice; equivalent phenotypic differences were present in samples from 9-wk-old female mice (unpublished data).

Quantitative measurements substantiated these observations: the mean cross-sectional area of collagen fibrils was increased in *Thbs1*$^{-/-}$ mice in both tissues, corresponding to mean fibril diameters of 124 nm for wild-type dermis, 138 nm for *Thbs1*$^{-/-}$ dermis, 192 nm for wild-type tail tendon, and 207 nm for *Thbs1*$^{-/-}$ tail tendon. *Thbs1*$^{-/-}$ tail tendons contained more large fibrils (>70,000 nm^2) and fewer intermediate fibrils (40,000–70,000 nm^2; Figure 1C). In both tissues, the range of fibril areas was increased in *Thbs1*$^{-/-}$ mice, as was the representation of large fibrils (upper quartiles in Figure 1, D and E). The frequency of small fibrils (lowest quartile) was unchanged (Figure 1, D and E). Thus absence of TSP1 affects the organization of collagen fibril ECM in different tissues.

Molecular determinants within the L-lectin domain control ECM deposition of a TSP1 C-terminal minitrimer

To begin to identify the mechanism by which TSP1 contributes to collagenous ECM organization, we turned to a model assay that measures ECM (defined in the assay as the insoluble material remaining after extraction of cell cultures with 20 mM ammonium hydroxide) accumulation of a monomeric red fluorescent protein (mRFP)–tagged, TSP1 C-terminal minitrimer protein (mRFPovTSP1C; Figure 2A). This protein contains the domains necessary and sufficient for ECM incorporation (Adams *et al.*, 2008). Endogenous TSP1 accumulates in ECM in the form of arrays of small puncta, and cells transfected to express mRFPovTSP1C also secrete and deposit this protein in the form of puncta in their ECM. A control, secreted mRFPo protein does not enter the ECM (Adams *et al.*, 2008). ECM accumulation of mRFPovTSP1C depends in part on the double calcium ion–binding site in the L-lectin domain, motif D1001DD (Adams *et al.*, 2008; Figure 2B). In other L-type lectin domains—for example, those of mammalian endoplasmic reticulum cargo transport proteins—ligand binding is mediated jointly by a calcium ion–binding site and an adjacent surface-exposed loop (Satoh *et al.*, 2007). The structurally homologous portion of the TSP1 L-lectin domain is the β7/β8 loop (Figure 2B), which contains eight surface-exposed residues with externally facing side groups. The possible functional significance of each of these for ECM incorporation activity was examined by alanine or charge-reversal point mutations. Mutation of T1032 or Y1040 had no effect on ECM incorporation, and mutation of N1033 or Q1038 had minor effects (Figure 2C). Mutation of either Y1029 or W1030 decreased ECM deposition by ~50% (Figure 2C). The strongest effects were obtained upon mutation of either D1031 (either to alanine or with charge reversal to arginine) or R1036; these mutations decreased ECM deposition by ~70% (Figure 2C). The transfections under matched conditions yielded equivalent percentages of mRFP-positive cells upon expression of either wild-type mRFPovTSP1C or the point mutant proteins (Supplemental Figure S1A). Quantification of immunoblots of the conditioned media from multiple independent experiments demonstrated that the point mutant proteins were present in conditioned media at equivalent levels to the wild-type protein (Supplemental Figure S1, B and C). Thus the reduced incorporation of some mutants into ECM is due to specific impairment of postsecretion processes.

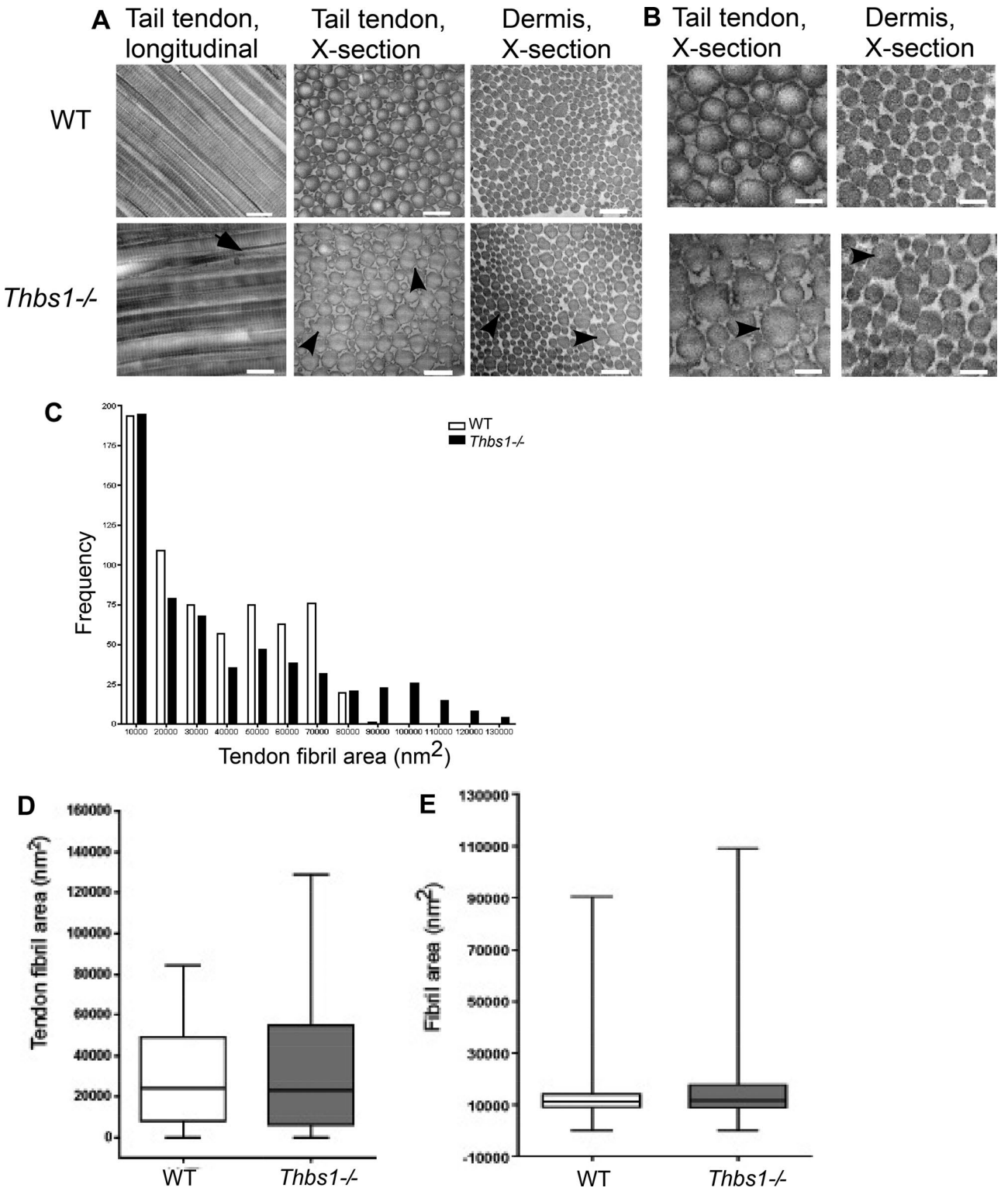

FIGURE 1: Tissues of *Thbs1*$^{-/-}$ mice contain disorganized collagen fibrils. (A, B) Transmission electron microscope images of collagen fibrils in the tail tendons or dermis of wild-type or *Thbs1*$^{-/-}$ C57BL/6 male mice at 6.5 wk of age. Arrowheads indicate splaying and splitting of collagen fibrils (in longitudinal section) and irregular, enlarged profiles of fibrils (in cross section) in *Thbs1*$^{-/-}$ mice. Bars, 500 nm (A), 200 nm (B). (C) Frequency histogram of the cross-sectional areas of tail tendon fibrils. In each wild-type or *Thbs*$^{-/-}$ sample, 8–10 images were scored containing 250–650 fibrils/image. (D, E) Box-and-whisker plots demonstrate that the range of fibril areas and representation of fibrils with large areas (upper quartile) is increased in tail tendon (D) or dermis (E) of *Thbs1*$^{-/-}$ mice.

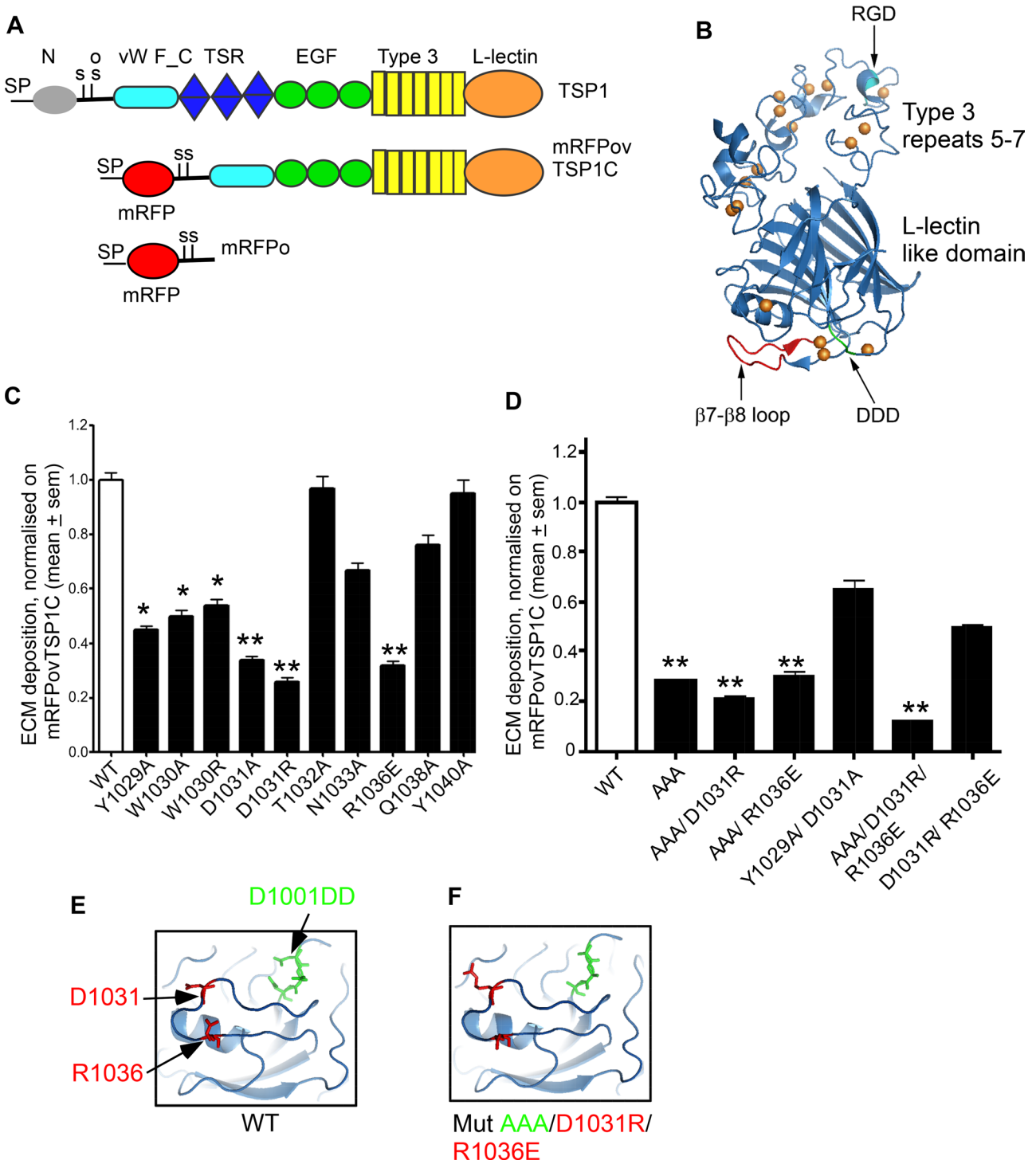

FIGURE 2: Identification of joint roles of the β7/8 loop and double calcium ion–binding site in the L-lectin domain of TSP1 in ECM incorporation of mRFPovTSP1C. (A) Schematics of the domain organization of the TSP1 polypeptide, mRFPovTSP1C, and the control mRFPo. EGF, epidermal growth factor–like domain; N , N-terminal domain; o, oligomerization domain; SP, signal peptide; vWF_C, von Willebrand factor type C domain; TSR, TSP type 1 domain. (B) Structure of the L-type lectin domain of TSP1 from Protein Data Bank 1UX6. The ECM incorporation activity site includes the DDD motif and β7/β8 loop and is at the outer tip of the domain, remote from the RGD motif that is in the last type 3 repeat. (C) Identification of single point mutations that decrease ECM accumulation activity of mRFPovTSP1C, scored as described in *Materials and Methods*. (D) Identification of a multiple point mutation that maximally inhibits ECM accumulation of mRFPovTSP1C. In each graph, data are shown as mean ± SEM. *$p \leq 0.001$ and **$p \leq 0.0001$ relative to wild-type control. (E, F) Enlarged view of the region of the TSP1 L-lectin domain around the novel ECM incorporation activity site, showing the polypeptide backbone and side groups of the identified key residues in wild type (E) and homology modeling of the AAARE mutations (F).

To achieve more complete inhibition of ECM deposition, we next tested combined point mutations. These included pairwise combinations of point mutations within the β7/β8 loop or combinations of these with the D1001DD-to-A1001AA mutation (termed AAA), which partially blocks ECM incorporation (Adams *et al.*, 2008; Figure 2D). Combinations such as Y1029A/D1031A or D1031R/R1036E did not further inhibit ECM incorporation (Figure 2D; unpublished data), and the AAA/D1031R or AAA/R1036E combinations had similar effects to that of AAA alone. However, accumulation of mRFPovTSP1C/AAA/D1031R/R1036E in ECM was diminished to ~10% of wild type (Figure 2D). The residual deposits were amorphous and covered much smaller areas than those formed by mRFPovTSP1C. Thus both puncta assembly and ECM accumulation were impaired. The transfections under matched conditions yielded equivalent percentages of mRFP-positive cells upon expression of either wild-type mRFPovTSP1C or the combination point mutant proteins (Supplemental Figure S1D). The combination mutant proteins were present in conditioned media at equivalent levels to wild-type mRFPovTSP1C (Supplemental Figure S1, E and F). The reduced ECM accumulation of the AAA/D1031R/R1036E mutant was confirmed in a second cell type, CHO (Supplemental Figure S1, G and H). Residues D1031 and R1036 are surface exposed on opposite sides of the β7/β8 loop near its outer tip (Figure 2E). We examined by homology modeling whether either mutation is predicted to affect the tertiary structure of the L-lectin domain. Molecular dynamics modeling showed that the alterations to the side groups at the D1031 and R1036 positions or the D1001DD to AAA mutation did not affect the folded protein conformation (Figure 2F; unpublished data). The AAA mutation does not affect secondary structure (Adams *et al.*, 2008).

The novel L-lectin–domain site mediates ECM incorporation of intact TSP-1

Having identified this novel site in the L-type lectin domain, our next step was to test the functional significance of the AAA/D1031R/R1036E mutations (abbreviated AAARE) in the context of full-length TSP1 (Figure 3A). ECM deposition was visualized with two antibodies, reactive with epitopes in the laminin G–like N-terminal domain (N) or the type 3 repeats (T3), respectively. Very similar results were obtained with both antibodies. ECM accumulation of TSP1/AAARE was decreased by 60–70% relative to wild-type TSP1, as established by immunofluorescence (Figure 3, B–D) or immunoblotting of the ECM (Figure 3, E and F, shown for the T3 antibody only). ECM deposition of fibronectin remained unaltered under the different conditions (Figure 3, E and G). Because the N-terminal half of TSP1 contains multiple heparin-binding sites and conformation flexibility of the TSP-1 molecule has been documented (Tan *et al.*, 2006; Calzada *et al.*, 2008), we considered whether heparin-binding sites in the N and TSR domains might work together in intact TSP1 to increase the avidity of ECM incorporation. We compared directly the ECM deposition activity of TSP1, TSP1/AAARE, No (amino acids [aa] 1–297 of TSP-1), NovTSR (aa 1–530), and NoC minitrimer (aa 1–297 plus 531–1152; Figure 3A), all detected with an antibody to the N domain. Only the NoC protein had similar ECM incorporation activity to TSP1 itself (Figure 3, B and C). ECM deposition of No or NovTSR was only in small patches (Figure 3B) and represented no more than 20% of the level of either TSP1 or NoC (Figure 3C), even though all the proteins were expressed equivalently (Figure 3D). These results show that the vWF_C and TSR domains do not mediate ECM incorporation of TSP1, whereas the N domain contributes at a low level.

A homologous L-lectin–domain site controls ECM accumulation of TSP5/COMP

The DDD motif is invariant in vertebrate TSPs, and the R1036 position is also very strongly conserved (Figure 4). To determine whether the newly identified L-type lectin domain site is important for ECM accumulation of other TSPs, we examined the pentameric family member TSP5, which is a component of cartilage ECM and has a simpler domain organization without the N-terminal, vWF_C, or TSR domains (Posey *et al.*, 2008; Figure 5A). Endogenous TSP5 was incorporated into ECM of chondrosarcoma cells as arrays of puncta, some of which align with fibrillar elements (Figure 5B). Ectopic TSP5 deposited by COS7 cells also appeared as arrays of puncta (Figure 5B). Mutation of Q623 or R628 individually (the residues in TSP5 equivalent to D1031 and R1036; Figure 4) had little or no effect on ECM accumulation (Figure 5C). An R628E mutant, alone or in combination with Q623E, reduced ECM accumulation by ~20% (Figure 5C). The TSP5/D593DD/AAA mutant was 70% reduced for ECM accumulation, and inclusion of the Q623E and R628E mutations with D593DD/AAA resulted in a statistically significant further decrease in ECM deposition to 10% that of wild-type TSP5, with residual deposits appearing amorphous, with greatly diminished puncta (Figure 5, B and C). The decreased deposition of TSP5 mutants in ECM was confirmed by immunoblotting of ECM (Figure 5D). The transfections under matched conditions yielded equivalent percentages of V5-positive cells for the wild-type or mutant TSP5 proteins (Supplemental Figure S2A). The mutant TSP5 proteins oligomerized correctly (Supplemental Figure S2B; oligomerization shown for TSP5 only) and were present at equivalent levels to those of wild-type TSP5 in conditioned media (Supplemental Figure S2C). We conclude that the DDD site has general functional significance for ECM deposition and puncta assembly of TSPs, with more varied roles of the "D" and "R" positions. Of interest, many TSP5 mutations that are causal for PSACH result in buildup of mutant TSP5 and other ECM molecules within the endoplasmic reticulum of chondrocytes, suggesting that although secretion is impaired, ECM interaction site(s) are not (Merritt *et al.*, 2007). COS cells can secrete these mutant TSP5 proteins (Chen *et al.*, 2004), and therefore we analyzed the ECM accumulation of a prevalent PSACH mutation, TSP5/ΔD469 (Posey *et al.*, 2004). This protein was secreted effectively (Supplemental Figure S2C) and accumulated as puncta in ECM to the level of wild-type TSP5, clarifying that the ΔD469 PSACH mutation does not intrinsically impair ECM accumulation activity (Figure 5C).

The mechanism of ECM accumulation of TSP molecules depends on L-lectin domain–dependent intermolecular recruitment

On the basis of the general importance of the novel L-lectin domain site for ECM accumulation of TSP1 and TSP5, our next goal was to identify how this site mediates ECM incorporation. We first considered that the TSP L-lectin domain might bind a sugar group. However, tests of mRFPovTSP1C against the Functional Glycomics Consortium microarray of 406 glycans did not reveal any significant binding either in absence or presence of calcium ions (unpublished data). We next considered that ectopic expression of the TSP1 or TSP5 proteins might affect cell proliferation or viability, thereby altering parameters of ECM deposition indirectly. However, expression of wild-type or mutant TSP1 or TSP5 proteins did not result in altered cell growth over the time period of the experiments (Supplemental Figure S3).

We therefore initiated pilot comparative proteomics of the ECM deposited by cells expressing mRFPo, mRFPovTSP1C, or mRFPovTSP1C/AAARE to identify any changes in the composition of the

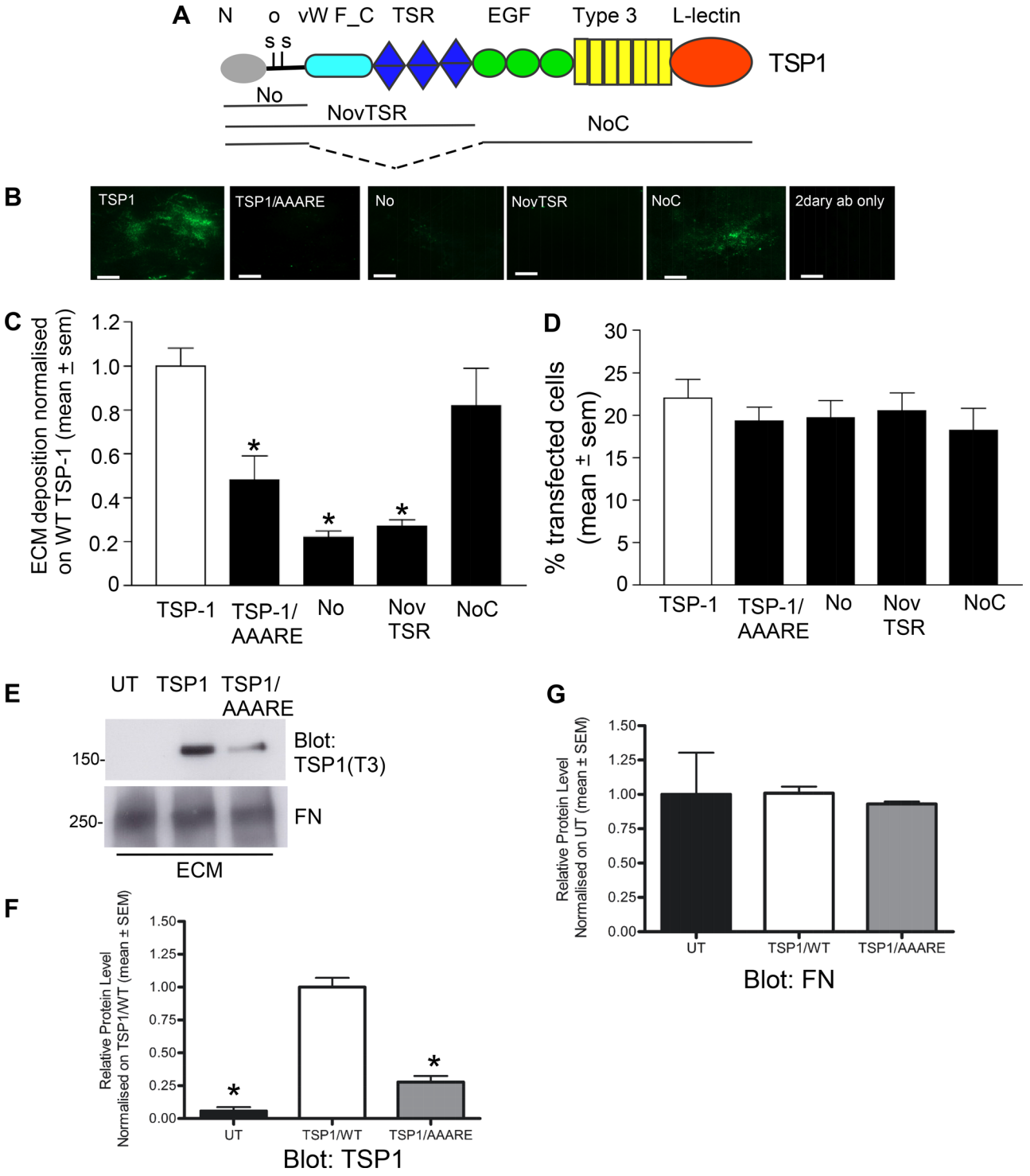

FIGURE 3: Major role of the L-type lectin–domain site in ECM accumulation of intact TSP1. (A) The domain organization of TSP1 showing the domains included in different constructs. C, TSP C-terminal region; N, N-terminal domain; o, oligomerization domain; v, von Willebrand factor C domain. (B–D) ECM accumulation activity of TSP1 compared with TSP1/AAARE mutant and N- and C-terminal minitrimers. COS-7 cells were transfected with the indicated constructs and ECM accumulation quantified 4 d later by staining all samples with antibody to TSP1 N domain. (B) Examples of the ECM deposition patterns of the TSP1-derived proteins. Bars, 20 µm. (C) Quantification of ECM deposition relative to wild-type TSP1 from multiple immunofluorescence experiments. *$p \leq 0.01$ relative to wild-type control. (D) Equivalent expression of the proteins. Cells were fixed in 2% paraformaldehyde, permeabilized, and stained with antibody to TSP1 N domain. (E) Immunoblots demonstrating reduced ECM accumulation of TSP1/AAARE mutant. UT, untransfected control cells. (F, G) Quantified data on TSP1, TSP1/AAARE, and fibronectin accumulation in ECM from multiple immunoblots. In F, *$p \leq 0.001$ relative to wild-type in ECM. In C, D, F, and G, data are shown as mean ± SEM.

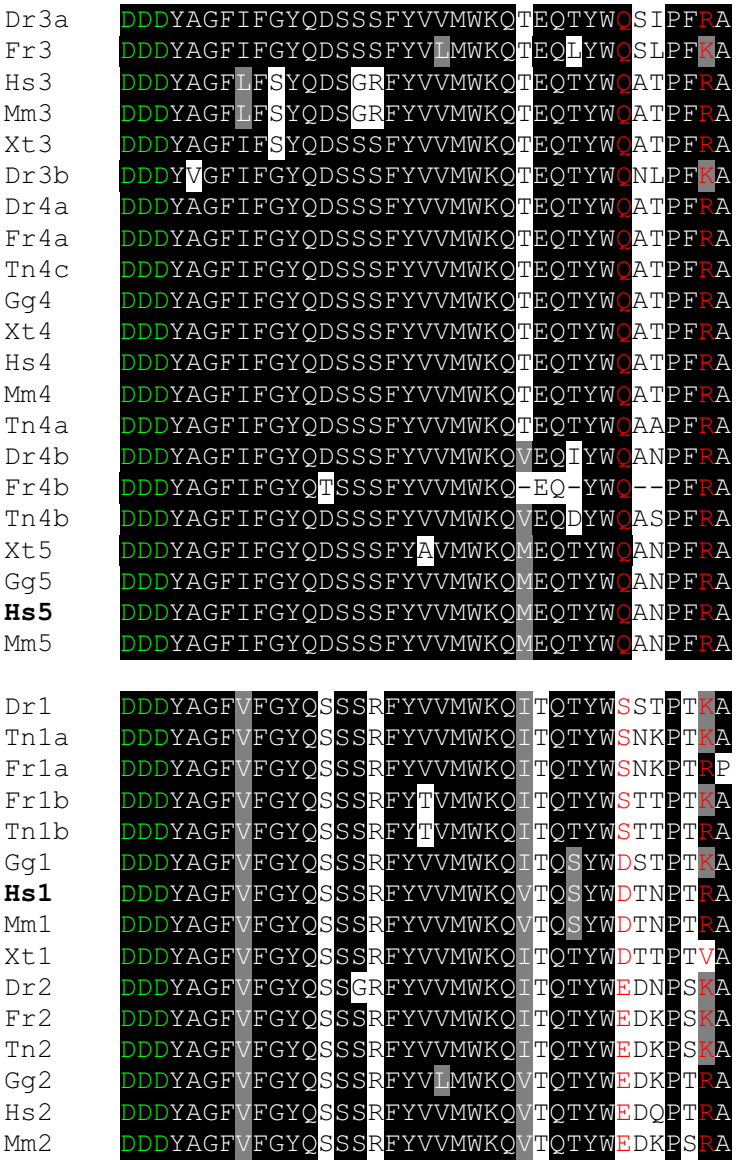

FIGURE 4: Multiple sequence alignment of the DDD motif and β7/β8 loop region of the TSP L-lectin domain from vertebrate thrombospondins. A TCOFFEE multiple sequence alignment of the region corresponding to human TSP1 aa 1001–1037 from the thrombospondins of representative vertebrates is presented in Boxshade 3.2. Black shading indicates identical residues, gray shading indicates conservative substitutions, and white background indicates unrelated amino acids. The DDD motif is in green, and the residues corresponding to D1031 and R1036 of human TSP1 are in red. Sequences used for the alignment correspond to those in Bentley and Adams (2010), with correction of the Xt5 sequence on the basis of expressed sequence tags. Dr, *Danio rerio*; Gg, *Gallus gallus*; Hs, *Homo sapiens*; Mm, *Mus musculus*; Tn, *Tetraodon nigriviridis*; Tr, *Takifugu rubripes*; Xt, *Xenopus tropicalis*.

ECM. The analysis focused on bands that appeared enriched upon SDS–PAGE analysis of the ECM from cells expressing mRFPovTSP1C. Surprisingly, the protein most enriched in the ECM of cells expressing mRFPovTSP1C was endogenous TSP1, as identified by peptides from the N-terminal domain, which is not included in mRFPovTSP1C (Figure 2A). From one protein band enriched in the ECM from cells expressing mRFPovTSP1C, 17 peptides from TSP1 were obtained, of which 11 were derived from the N-terminal domain, aa 1–240. The corresponding region of the lane in which ECM from cells expressing mRFPovTSP1C/AAARE was run yielded 19 peptides from TSP1, of which 1 was derived from the N-terminal domain. Minor enrichment of perlecan and decorin was also noted in the analysis (unpublished data). This pilot finding raised the novel hypothesis that the incorporation of TSP1 into ECM depends on a *trans*-acting property of the L-lectin domain—for example, mediation of intermolecular interactions. To test this idea, we first compared the dose–response characteristics for ECM incorporation of mRFPovTSP1C or mRFPovTSP1C/AAARE. ECM incorporation of mRFPovTSP1C was dose dependent, whereas mRFPovTSP1C/AAARE incorporation was minimal at all amounts of transfected plasmid tested (Figure 6A). Conditions for intermediate incorporation of mRFPovTSP1C (48% of maximum) were chosen to test how its expression affected accumulation of endogenous TSP1 into ECM. Under each experimental condition, the ectopically expressed proteins were detected in conditioned media (Figure 6, B and C), and the low level of endogenous TSP1 in conditioned media was unchanged (Figure 6, B and D). Endogenous TSP1 in ECM was identified specifically by immunoblot with antibody to the N-terminal domain, and, as reported previously, was barely detectable in the ECM of untransfected COS7 cells (Figure 6E, lane 1; quantified in Figure 6F). In agreement with the pilot proteomics, endogenous TSP1 accumulated in the ECM of cells expressing mRFPovTSP1C but not in the ECM of cells expressing control mRFPo or mRFPovTSP1C/AAARE (Figure 6, E, lanes 2–4, and F). Similar results were obtained by immunoblotting with antibody to the type 3 repeats of TSP1 (Figure 6E). As expected, mRFPovTSP1C accumulated in ECM and mRFPovTSP1C/AAARE did not (Figure 6, E and G). The elevated ECM content of endogenous TSP1 in the presence of mRFPovTSP1C had specificity, because ECM deposition of endogenous fibronectin was unchanged irrespective of the transfected protein (Figure 6, E and H). Immunofluorescence of isolated ECM confirmed that endogenous TSP1 was specifically enriched only in the ECM of mRFPovTSP1C-expressing cells. Examples of colocalized or closely opposed TSP1 puncta and mRFPovTSP1C puncta were observed (Figure 6I, arrow). The lack of complete colocalization is probably because it will be a random event whether a TSP1 molecular interacts extracellularly with another TSP1 molecule or with an mRFPovTSP1C molecule or vice versa. These data are consistent with a mechanism of L-lectin domain–dependent recruitment of endogenous TSP1 as puncta into the insoluble ECM.

Because of the high conservation of the L-lectin domain site across the TSP family (Figure 4), we examined whether TSP5 also had *trans*-recruitment activity. Because TSP5 is a natural "mini-TSP" with no N domain, an additional expression construct for full-length TSP5 with Flag and myc tags was developed

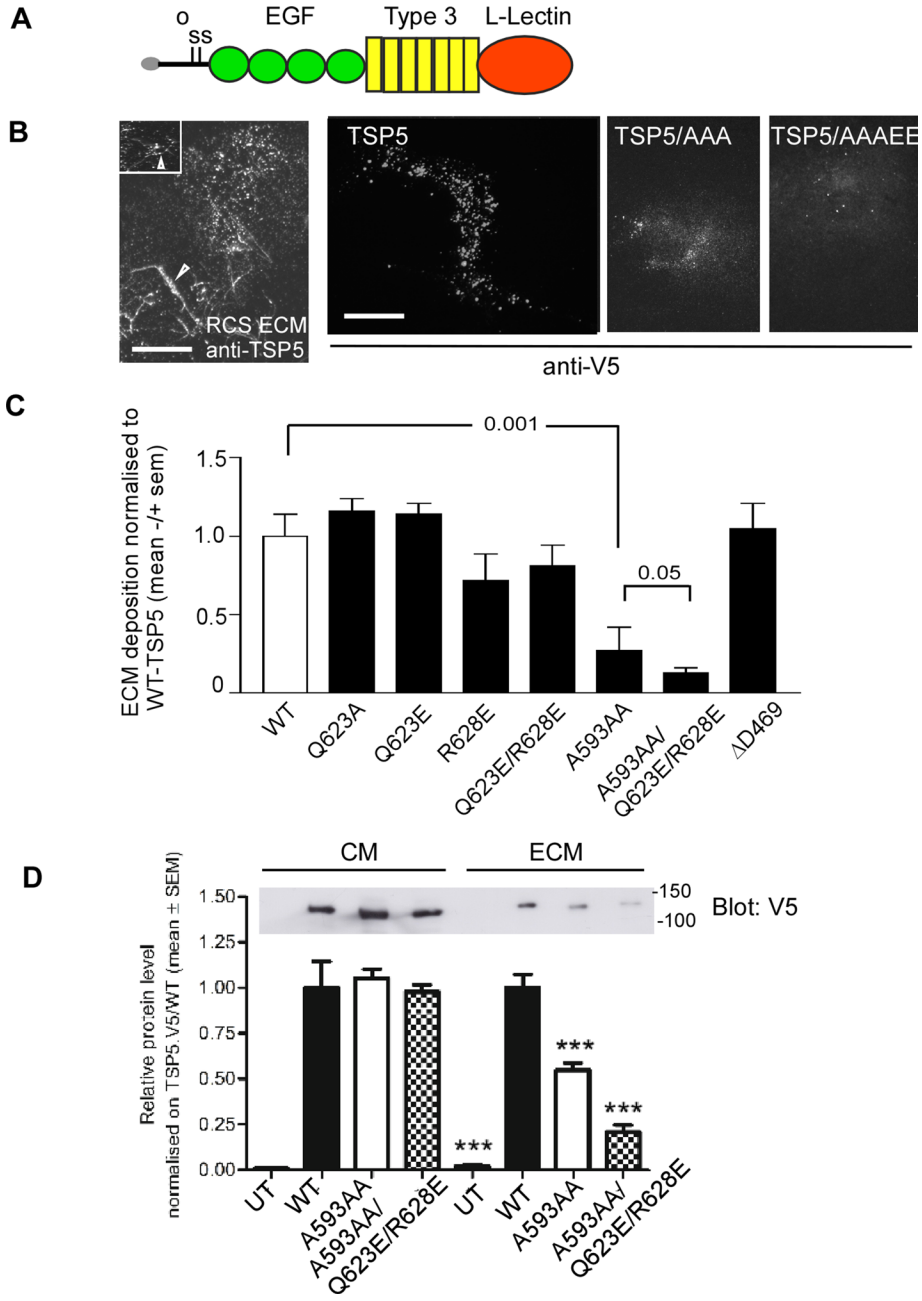

FIGURE 5: The L-type lectin–domain site has conserved activity in ECM accumulation of thrombospondin5. (A) Domain organization of TSP5. Key as in Figure 1 legend. (B–D) ECM accumulation activity of wild-type TSP5 compared with point mutations of its L-type lectin domain. (B) Immunofluorescence detection of endogenous TSP5 puncta in ECM produced by RCS cells (left) or V5-tagged forms of TSP5 expressed in COS-7 cells (right three panels). (C) Quantified comparison of ECM deposition of TSP5, the L-type lectin domain mutants, and a PSACH mutant, TSP5ΔD469. All proteins were detected with antibody to V5 epitope tag. (D) Representative V5 immunoblot and quantified analysis of ECM accumulation of TSP5/AAA and AAAEE mutants from V5 immunoblots. In C and D, data are shown as mean ± SEM from four experiments. ***$p < 0.001$ by one way ANOVA vs. TSP5.V5.

(Supplemental Figure S4, A and B). Wild-type and mutant TSP5 with V5 tags, or FlagTSP5Myc, were each expressed ectopically in separate cell populations to avoid cotranslational co-oligomerization. Cells were then trypsinized, washed extensively, and plated 24 h later as either single populations of cells expressing each protein or pairwise 1:1 mixtures of cells transfected with the different TSP5 expression plasmids. Wild-type and mutant V5-tagged proteins were present at very similar levels in conditioned media from each experimental condition, yet only TSP5.V5 was significantly enriched in ECM after coculture (Figure 7, A and B). FlagTSP5Myc was also secreted effectively and yet was enriched in ECM only when TSP5.V5 was also present in the medium. In the presence of TSP5/Mut.V5, deposition of FlagTSP5Myc was not significantly altered from the single-expression control (Figure 7, A and C). Thus the L-lectin domain motif of TSP5 also functions in intermolecular recruitment of TSP5 molecules into ECM.

Because TSP1 is present at low levels in cartilage and tendon along with TSP5 (DiCesare *et al.*, 1994) and *Thbs1*$^{-/-}$ mice have altered collagen fibril organization in tendons (Figure 1), we tested whether TSP1 and TSP5 could recruit each other into ECM in an L-lectin domain–dependent manner. Under transfection conditions for low-level ECM deposition of either TSP1 or TSP5.V5, conditioned media and ECMs were analyzed with the appropriate specific antibodies. ECM incorporation of TSP5.V5 was strongly and specifically increased in the presence of expressed TSP1 (Figure 7D, top, right; quantified in Figure 7E). Incorporation of TSP5/AAAEE.V5 was minor in the presence of TSP1 and was barely detectable in the presence of TSP1/AAARE (Figure 7D, top, right; Figure 7E). TSP1 was incorporated at similar levels into ECM in the presence of either TSP5.V5 or TSP5/AAAEE.V5 (Figure 7D; quantified in Figure 7F). In contrast, TSP1/AAARE incorporated weakly when coexpressed with either wild-type or mutant TSP5.V5 (Figure 7D, bottom, right; Figure 7F). Thus ECM recruitment can also take place between trimeric and pentameric TSPs, and the putative intermolecular recruitment activity of the L-lectin domain motif is important in this process.

TSP molecules undergo direct interactions in *trans*

To elucidate the mechanism underlying this intermolecular activity of the L-lectin domain of TSPs, we first considered the possible role of fibronectin as a bridging molecule between TSP molecules in the ECM. Fibronectin enhances matrix assembly of several ECM components in cell culture (Sabatier *et al.*, 2009) and is present in ECM in our experiments (e.g., Figure 4). However, addition of a 10-fold excess of fibronectin to the cells (based on quantification of endogenous fibronectin in ECM by immunoblots calibrated against known amounts of purified fibronectin) did not alter the amount of TSP1 incorporated into ECM. Addition of excess soluble collagen I was also ineffective (unpublished data).

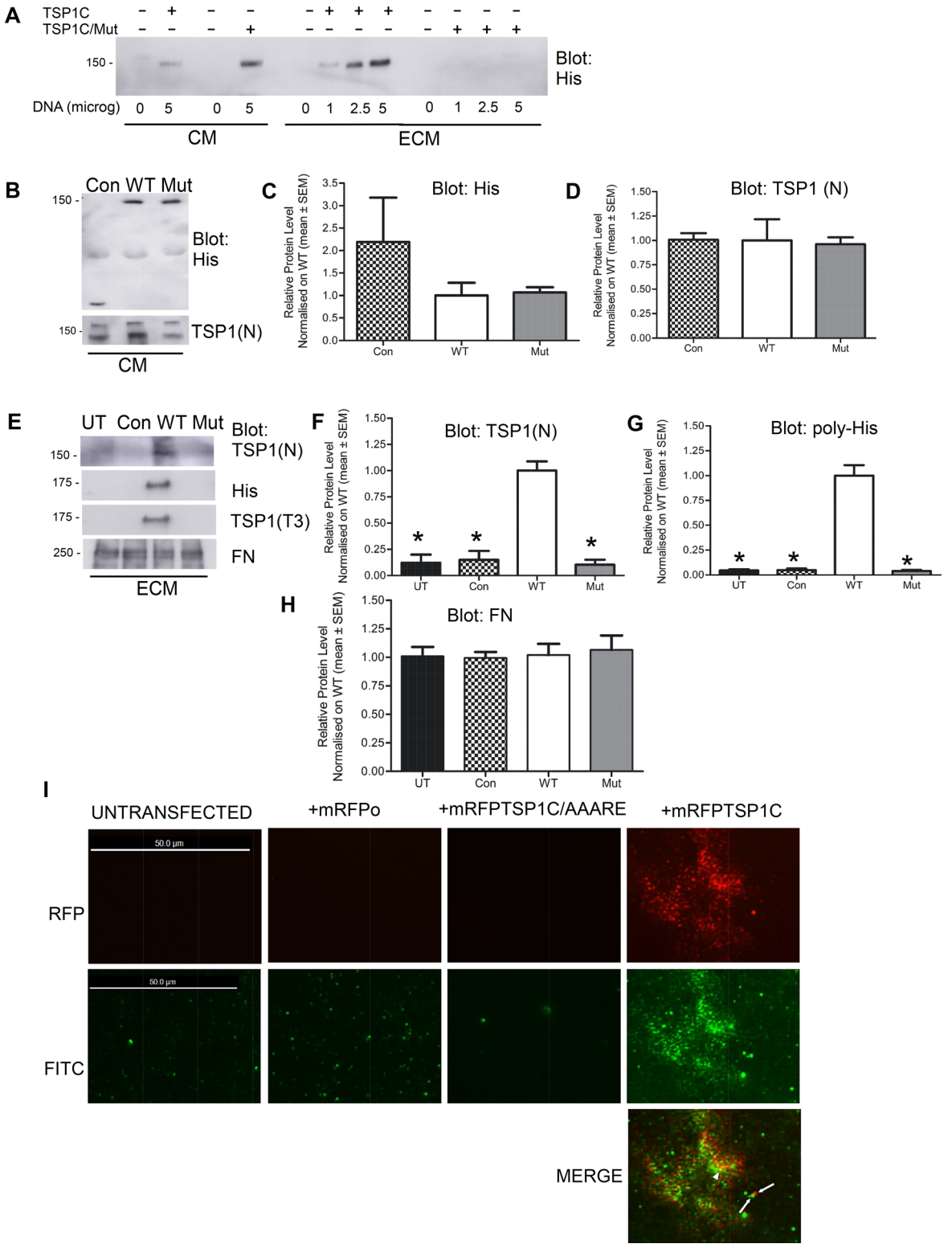

FIGURE 6: A *trans*-acting intermolecular mechanism of the L-type lectin domain site controls ECM accumulation of TSP1. (A) Demonstration of experimental conditions for specific concentration-dependent ECM accumulation of mRFPovTSP1C. ECM was analyzed 3 d after transfection by immunoblot for the hexahistidine tag. CM, conditioned medium. (B–D) Minitrimers and endogenous TSP1 are present in conditioned medium at equivalent levels under each experimental condition. (E–G) Endogenous TSP1 (detected with N-terminal domain–specific TSP1 antibody; also antibody A6.1 to T3 repeats) is enriched only in the ECM of mRFPovTSP1C-expressing cells. ECM incorporation of fibronectin was unaltered (E, H). In C, D, and F–H, data are shown as mean ± SEM. In F and G, *$p \leq 0.0001$ vs. wild-type value by one-way ANOVA. (I) Specific colocalization of endogenous TSP1 (detected with N-terminal–domain specific antibody; FITC panel) with expressed mRFPovTSP1C (RFP panel) within ECM. Arrowhead indicates example of colocalization, and arrows an apposition of puncta.

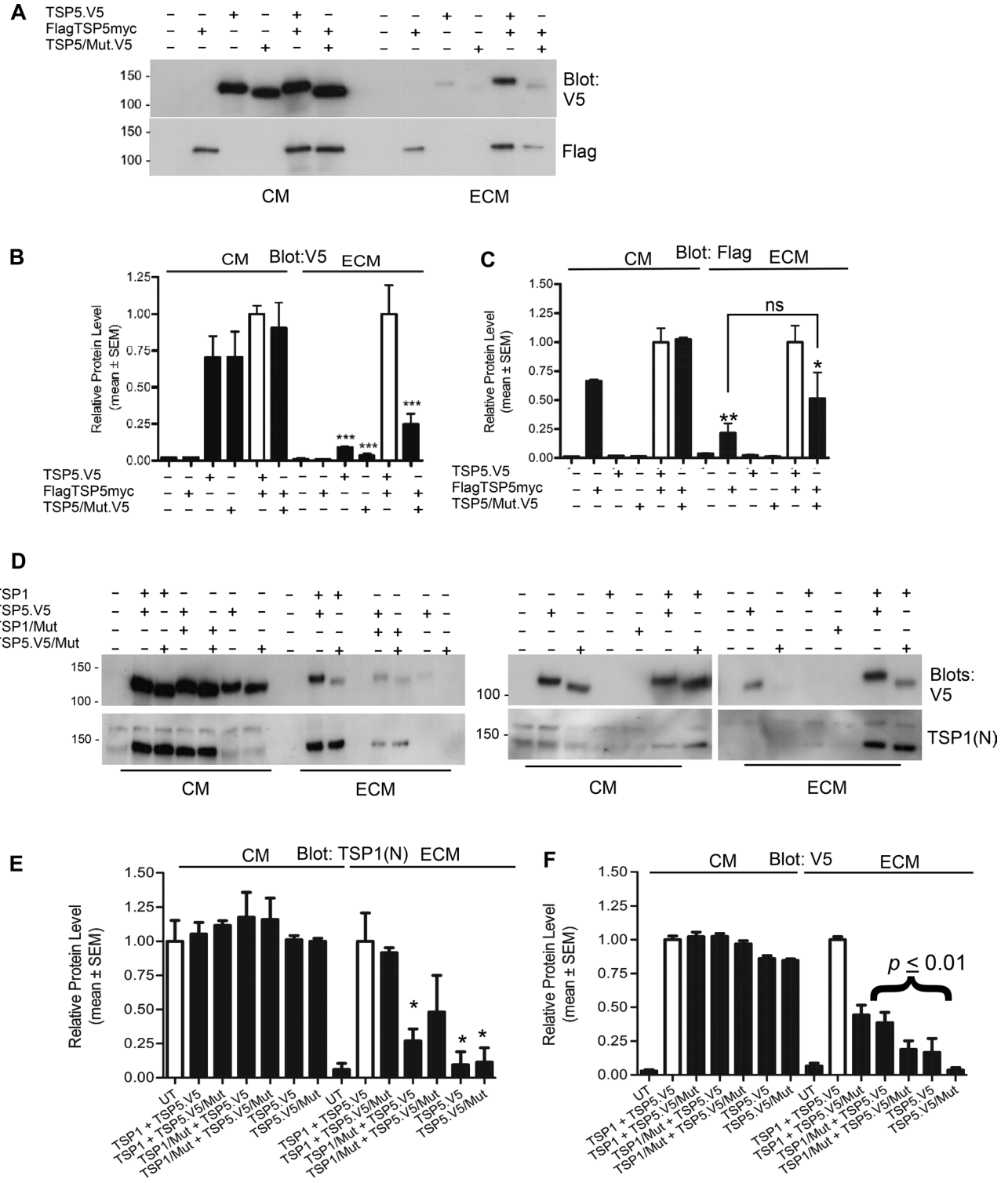

FIGURE 7: Intermolecular ECM accumulation activity is conserved in TSP5 and also acts heterotypically. (A–C) L-lectin domain–dependent corecruitment of TSP5 molecules into ECM. Transfections were as indicated. TSP5.V5 and TSP5/AAAEE.V5 are present at equivalent levels in conditioned medium (CM), but only TSP5.V5 is enriched in ECM upon coculture with cells expressing FLAGTSP5myc. Similarly, FLAGTSP5myc is enriched in ECM only in the presence of TSP5.V5. (A) Immunoblot. (B, C) Quantification and normalized data, shown as mean ± SEM. *$p < 0.05$, **$p \leq 0.001$, and ***$p \leq 0.0001$ by one-way ANOVA against the TSP5.V5 plus FlagTSP5myc ECM condition. (D–F) L-lectin domain–dependent corecruitment of TSP1 and TSP5 into ECM. (D) Transfection conditions were as indicated, and full-length TSP5 proteins were detected by V5 tag (top). Full-length TSP1 was detected with antibody to its N-terminal domain (bottom). (E, F) Quantified and normalized data, shown as mean ± SEM. In E, *$p \leq 0.001$ by one-way ANOVA against the TSP1 plus TSP5.V5 ECM condition.

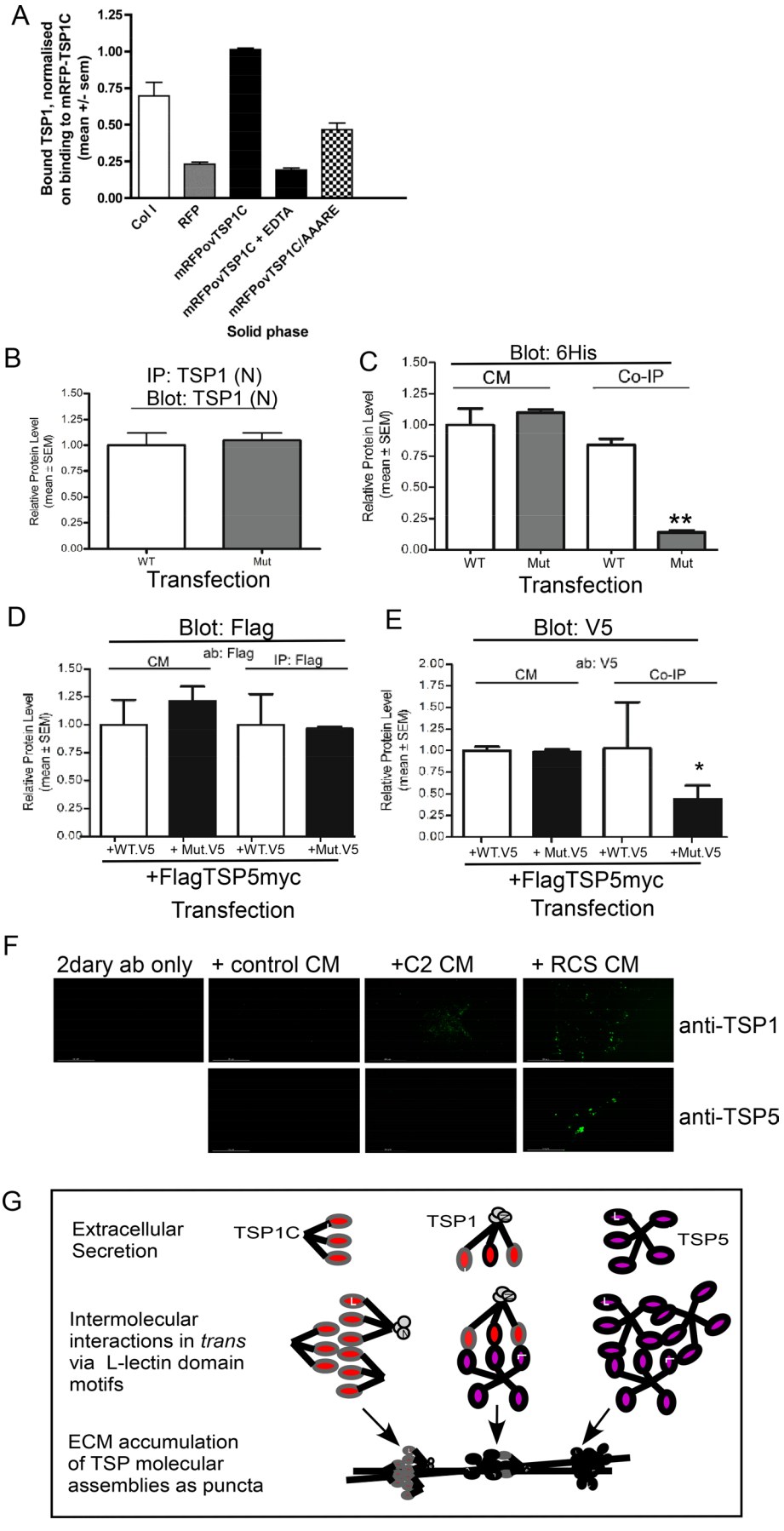

To test for possible direct, L-lectin domain motif–dependent interactions between TSP1 molecules, we set up an enzyme-linked immunosorbent-type protein-binding assay with TSP1. Collagen I, which binds relatively weakly to TSP1 (Cockburn and Barnes, 1991), RFP control protein, or wild-type or mutant mRFPovTSP1C proteins were absorbed to wells, blocked, and overlaid with purified full-length TSP1, and the binding of TSP1 detected was specifically with antibody to TSP1 N domain. TSP1 binding to collagen I or mRFPovTSP1C was significantly elevated over basal binding to RFP, whereas binding to mRFPovTSP1C/AAARE was not. Interaction with mRFPovTSP1C was inhibited in the presence of EDTA, demonstrating the importance of calcium-replete TSP1 for the interaction (Figure 8A).

TSPs secreted by cells also undergo *trans* interactions in solution

Because the results of the foregoing binding assay implied that TSPs might also undergo *trans* interactions in solution, their interactions were investigated further in the conditioned media of transfected cells. On immunoprecipitation of endogenous TSP1 (Figure 8B), mRFPovTSP1C, but not mRFPovTSP1C/AAARE, was coimmunoprecipitated (Figure 8C). Collagen I was not detected in the immunoprecipitates (unpublished data).

FIGURE 8: The L-lectin domain site functions in direct interactions between TSP molecules. (A) Intermolecular interactions of TSP1 molecules in vitro. Each column represents the mean; bars indicate SEM. (B, C) Physical association of TSP1 molecules in *trans* detected by coimmunoprecipitation and immunoblotting from conditioned media (two experiments; $^{**}p < 0.01$). (D, E) Physical association of TSP5 molecules in *trans* detected by coimmunoprecipitation and immunoblotting from conditioned media pooled from cells expressing different tagged forms of TSP5 ($^{*}p < 0.05$). (F) Demonstration that incorporation of ECM puncta of endogenous TSP1 or TSP5 can be driven extracellularly. ECMs were prepared from COS7 cells after 48 h in standard media or with exposure to conditioned media from C2C12 or RCS cells and stained with antibodies to TSP1 or TSP5. Representative images from three independent experiments. (G) Model for the mechanism of initiation and ECM accumulation of TSP puncta by TSP1-TSP1, TSP5-TSP5, or heterotypic TSP1-TSP5 intermolecular interactions. L, L-type lectin domain; N, N-terminal domain. See *Discussion* for details.

Similarly, after mixing conditioned media from matched numbers of transfected cells expressing different tagged forms of wild-type or mutant TSP5 and immunoprecipitating for FlagTSP5Myc (Figure 8D), wild-type TSP5.V5 was effectively coimmunoprecipitated, whereas TSP5AAAEE.V5 was not, even though both proteins were present in the same amounts in the conditioned media (Figure 8, D and E). Thus L-lectin domain–dependent, TSP-TSP intermolecular interactions in *trans* can occur directly and in solution, that is, before incorporation into the insoluble ECM.

This point was investigated further in relation to extracellular interactions of endogenously expressed TSPs. As documented, COS7 cells, which secrete a low level of TSP1 that is insufficient for ECM incorporation (Figure 3) into their ECM (Figure 3) and do not express TSP5 (see later discussion), were treated for 48 h with filtered conditioned media from mouse skeletal myoblastic C2C12 cells that endogenously express TSP1 (Adams *et al.*, 2008) or from rat chondrosarcoma (RCS) cells that endogenously express TSP5 (Figure 5). The isolated ECMs were then stained with antibodies for detection of TSP1 or TSP5. In comparison to the control condition in which neither TSP1 nor TSP5 was detected in ECM, punctate arrays of TSP1 were present in the ECM after treatment with either C2C12 or RCS medium. ECM deposition of TSP5 was detected only after treatment with RCS medium (Figure 8F). These results demonstrate that the concept that intermolecular interactions of TSPs facilitate their incorporation into ECM is relevant to endogenously produced TSPs and further establish that this step can take place extracellularly.

DISCUSSION

We demonstrate a novel molecular process of prospective general importance for ECM incorporation of TSPs. TSPs do not form structural fibrils in the ECM, and their functional significance for ECM organization has remained poorly understood and difficult to study. We demonstrate that the presence of TSP1 in collagenous ECM is relevant to collagen fibril organization in vivo. In the absence of TSP1, collagen fibrils in multiple mouse tissues are disorganized and enlarged, indicative of improper fibril organization. These phenotypes are clearly detectable in unchallenged mice, even though levels of TSP1 in postnatal dermis or tendon are low under normal physiological conditions (Kannus *et al.*, 1998; Pablos *et al.*, 1998). Similar alterations in collagen fibril packing and connective ECM organization have been described in tissues from *Thbs2*$^{-/-}$ or *Thbs5*$^{-/-}$ mice (Kyriakides *et al.*, 1998; Posey *et al.*, 2008, Alford *et al.*, 2013). *Thbs2*$^{-/-}$ mice have also been shown to suffer from skin laxity and weakened tail tendons (Kyriakides *et al.*, 1998). *Thbs4*$^{-/-}$ mice also show enlarged collagen fibrils in tendons and have reduced limb muscle grip strength (Frolova *et al.*, 2014). Loss of function of *Drosophila* TSP results in altered distribution of tiggrin, an ECM component required for proper ECM function at muscle–tendon attachment sites, and embryonic lethality (Subramanian *et al.*, 2007). Thus TSPs have significant conserved roles as modulators of ECM organization.

In analyzing the mechanisms by which TSPs affect ECM, a first requirement is to understand the molecular process by which TSPs accumulate in ECM. This process involves the deposition of TSPs as discrete, nanoscale puncta. We identify a novel site on the conserved TSP L-lectin domain in which specific residues of the β7/β8 loop work together with the calcium ion–binding DDD motif. We demonstrated the role of this novel site with regard to ECM incorporation of trimeric TSP1 and pentameric TSP5 and identified that the underlying molecular mechanism depends on L-lectin domain–mediated, intermolecular interactions in *trans* between TSP molecules. Both homotypic and heterotypic TSP interactions can occur. The evidence is that 1) ECM accumulation of endogenous TSP1 puncta is increased in the presence of mRFPovTSP1C minitrimer but not with mRFPovTSP1C/AAARE; 2) ECM accumulation of TSP5 puncta depends on the equivalent motif in the TSP5 L-lectin domain, and this also has intermolecular recruitment activity; 3) ECM accumulation of TSP5 is increased specifically in the presence of TSP1, yet this is not apparent for TSP5 mutated at the L-lectin domain site; 4) in vitro, direct binding in *trans* between TSP1 molecules depends on the L-lectin domain site; 5) physical association of TSP1 and mRFPovTSP1C, or between differently tagged forms of TSP5, in conditioned media is promoted by the L-lectin domain site; and 6) ECM incorporation of endogenous TSPs can also take place from conditioned media. With regard to the studied heterotypic interaction between TSP1 and TSP5, an interesting anomaly is the recruitment of TSP1 to ECM by both TSP5 and TSP5/AAAEE. Possibly, the additional L-lectin domain avidity provided by a pentameric cluster compensates for lack of appropriate charge or cation-dependent interactions at the ECM incorporation site of a trimer. Alternatively, the C-terminally located heparin-binding patch of TSP5 (Tan *et al.*, 2009) might be particularly accessible to cooperate with glycosaminoglycan binding by the N-domain of TSP1.

These unexpected findings lead to the novel concept that TSP molecules undergo intermolecular interactions via their L-lectin domain sites and that this activity is important for their ECM incorporation and assembly into puncta. Our model proposes that interactions between L-lectin domains of separate TSP molecules can be initiated in solution and lead to formation of multiprotein assemblies that incorporate in ECM in the form of TSP puncta (Figure 8D).

We also demonstrate that TSP1 affects collagen fibril organization in multiple tissues. Knowledge of mechanisms of TSP/collagen interactions is sparse; most data are from studies of TSP5. In tendon and cartilage ECM, TSP5 associates with collagen fibril bundles, with preference for the gap region; in vitro it promotes collagen fibrillogenesis (Sodersten *et al.*, 2005; Halasz *et al.*, 2007). In the dermis, TSP5 clusters are associated with collagens XII and XIV in the dermal–epidermal junction zone (Agarwal *et al.*, 2012). The novel site we identified is distinct from a collagen-binding peptide identified in the TSP5 L-lectin domain (Holden *et al.*, 2001) or known sites of disease-causing mutations in any TSP. We speculate that collagen interactions might further stabilize the ECM accumulation of TSP puncta by binding to a face of the L-lectin domain distinct from the site that we identified here, or to another TSP domain. This remains a question for further investigation.

The identification of this novel mechanism has broad implications for consideration of the biological roles of TSPs. TSP1 and TSP2 are present at very low levels in adult mammalian tissues, yet are elevated extracellularly due to release by multiple cell types during wound repair or in contexts such as atherosclerotic lesions, breast tumor stroma, or fibrosis (Agah *et al.*, 2002; Stenina *et al.*, 2007; Yee *et al.*, 2009). The process of "matrix trapping" of TSPs into ECM according to L-lectin domain–mediated *trans* interactions dependent on their local concentration would imply that increased levels of TSPs will be associated with a change in physiological presentation to localized, insoluble ECM deposits. Intrinsically, the activities and binding interactions of other TSP domains will become clustered and contribute to microenvironmental heterogeneity within the ECM. This model can explain how TSPs can participate in many tissues that vary widely in ECM composition. The possibility for heterotypic, as well as homotypic, L-lectin domain interactions demonstrates that "matrix trapping" can be a general principle in the TSP family. Conceptually, coexpression of several TSPs can enable intermolecular interactions between TSPs and for the lowest

expressed TSPs to be recruited into ECM by more abundant TSPs. Efforts to translate aspects of TSP biology to the clinic have focused on properties fulfilled by TSPs in solution (Zhang and Lawler, 2007; Isenberg *et al.*, 2009). We predict that the previously unknown basic mechanism identified here has important roles in TSP and ECM biology. Knowledge of this process brings new potential for approaches to control the localization and functionality of TSPs within the diverse ECMs of tissues.

MATERIALS AND METHODS

Cell lines and materials

Cos-7 cells, CHO cells, RCS cells, and C2C12 mouse skeletal myoblasts were cultured in DMEM containing 10% fetal calf serum. All cells were maintained at 37°C in a humidified 5% CO_2 atmosphere. pCEP-pu/mRFPovTSP1C, pCDNA3/TSP1, and pCDNA3/TSP5. V5His plasmids were as described (Adams *et al.*, 2008). TSP5 cDNA containing the ΔD469 mutation was the gift of Jack Lawler (Harvard Medical School, Boston, MA). Site-directed mutagenesis was carried out on TSP1 or TSP5 cDNA templates by PCR-based mutagenesis using oligonucleotides as listed (Supplemental Table S1) and the QuikChange II XL site-directed mutagenesis kit (Stratagene, La Jolla, CA). All oligonucleotides were synthesized by Sigma-Genosy (Gillingham, UK); oligonucleotides for mutagenesis reactions were HPLC purified. DNA sequences were confirmed by automated DNA sequencing by the Cleveland Clinic Foundation (CCF) Genomics Core or MWG Europe (Eurofins, Ebersberg, Germany). Primary antibodies used included rabbit polyclonal antisera to DsRed (Clontech, Palo Alto, CA), RFP (Abcam, Cambridge, UK), fibronectin (Sigma-Aldrich, St. Louis, MO), and TSP5/COMP (Kimiya Biomedical, Tukwila, WA); rabbit monoclonal to TSP5 (EPR6289; Abcam); mouse monoclonal antibodies to human TSP1 (MAI; Lawler *et al.*, 1985; a gift of Jack Lawler), A6.1 (Abcam), and FLAG tag (M2, Sigma-Aldrich, Gillingham, UK), V5 tag (Clontech, Saint-Germain-en-Laye, France), or hexahistidine tag (Genscript Piscataway, NJ, or Abcam) for immunoblotting; goat polyclonal anti–V5-fluorescein isothiocyanate (FITC; Abcam) for immunostaining; and goat anti-TSP1 N-domain (Santa Cruz Biotechnology, Santa Cruz, CA). Alkaline-phosphatase–conjugated and FITC-conjugated secondary antibodies were from Applied Biosystems (Carlsbad, CA) and ICN Biomedicals (Irvine, CA), respectively.

Bioinformatics and protein structure analysis

Predicted effects of point mutations of the TSP1 L-lectin domain on its structure were examined by homology modeling using the SWISS-MODEL server (swissmodel.expasy.org) and the Swiss-PDB Viewer program (Guex and Peitsch, 1997). Template structures were generated by substituting the point mutations into the protein sequence. Models were submitted to the Dali server (ekhidna.biocenter.helsinki.fi/dali_server) to compare their structural relationship to Protein Data Bank 1ux6. PyMOL (www.pymol.org) was used to illustrate the models.

ECM accumulation

Transfection of cells and epifluorescence microscopy scoring of mRFP-tagged proteins in ECM were carried out as described (Adams *et al.*, 2008). Full-length TSP1 proteins were detected by immunostaining with antibodies reactive with epitopes in the N-terminal domain (N-20, MAII) or type 3 repeats (A6.1; Annis *et al.*, 2006). TSP5 tagged with V5 epitope was detected with anti–V5-FITC. Two coverslips were scored for each condition per experiment. The percentage of transfected cells was measured after fixing in 2% paraformaldehyde and staining nuclei with 4,6-diamidino-2-phenylindole (DAPI). Transfected cells and total number of nuclei per field were counted from 20 random fields/coverslip either by direct scoring of cells expressing mRFP-tagged proteins or by indirect immunofluorescence with the appropriate primary antibody. ECM deposition was scored from 30 fields/coverslip by morphometry, and the mean area of deposition of each mutant protein was normalized to the appropriate wild-type control. Colocalization of mRFPovTSP1C and endogenous TSP1 was examined by isolating ECM from untransfected cells or cells transfected with mRFP-tagged proteins, staining them with antibody to the N-terminal domain of TSP1, and examining them by epifluorescence microscopy with appropriate filters. Deposition of endogenous TSPs from conditioned media was analyzed by plating 2.5×10^5 COS7 cells on glass coverslips in p60 dishes. After 3 h, cells were either continued in standard medium or exposed to 72 h conditioned medium from C2C12 or RCS cells, from which any cellular material had been removed by centrifugation at 1200 rpm for 5 min and filtration through low–protein binding, 0.22-μm-pore filter units (Millipore). Then 48 h later, ECM was isolated from all samples and stained by indirect immunofluorescence for either TSP1 or TSP5 or with FITC-conjugated secondary antibody only. For SDS–PAGE analysis of ECM, 5.3×10^5 COS-7 cells/90-mm dish were transfected with 0.5–6 μg of plasmid and cultured for 60 h. ECM was isolated by treatment with 20 mM NH_4OH for 5 min, copious washing with water, and scraping into hot SDS–PAGE sample buffer containing 100 mM dithiothreitol (DTT) for analysis by immunoblot. Digital scans of immunoblots were analyzed with ImageJ (National Institutes of Health, Bethesda, MD) for normalization of band intensities. Molecular mass markers are indicated in kilodaltons on all immunoblot panels. Between three and eight independent experiments were carried out.

Thrombospondin secretion and immunoprecipitation

Three days after transfection, TSP proteins were collected from conditioned media on TALON metal affinity resin (Clontech) or heparin-Sepharose (Amersham Biosciences, Sweden) as previously described (Adams *et al.*, 2008). Beads were washed three times in Tris-buffered saline (TBS) containing 2 mM $CaCl_2$ and protease inhibitor cocktail (Pierce) and collected by centrifugation. TSP1 was also immunoprecipitated from conditioned medium with TSP1 N-20 antibody bound to protein G–agarose (Zymed). TSP5 was immunoprecipitated with Flag or V5 antibodies. Bead-bound proteins were solubilized in boiling SDS–PAGE sample buffer with or without 100 mM DTT and analyzed by Western blotting with appropriate antibodies and enhanced chemiluminescence detection for their expression level and oligomerization status. Digital scans of the blots were analyzed in ImageJ for normalization of band intensities.

Protein purification

For purification of recombinant TSP proteins, COS-7 cells were adapted over 1 mo to serum-free VP-SFM medium (Life Technologies) supplemented with 4 mM glutamine. We seeded 4.4×10^6 COS-7 cells/150-mm dish (Corning) and transfected them 1 d later with 24 μg of plasmid/dish using 60 μl of Polyfect transfection reagent (Qiagen) according to manufacturer's instructions and with the addition of 20 ml of fresh VP-SFM medium to each dish after transfection. Medium was harvested and cells refed with fresh VP-SFM medium each day up to a total of 50 ml/dish. Protease inhibitor VIII cocktail (Calbiochem) was added to harvested conditioned medium, the medium centrifuged, and the supernatants passed over 300 μl of TALON metal affinity resin at 4°C. Each column was washed three times with 10 ml TBS/$CaCl_2$ and eluted three times with 300 μl of TBS/$CaCl_2$ containing 1 M imidazole over 1.5 h. Purified proteins were dialyzed using Disp-Biodialyzer (Nest Group) in dialysis buffer (0.8× TBS with

2 mM $CaCl_2$) and concentrated as needed by centrifugation in 50,000-Da cutoff Amicon Microcon Ultra YM filter units (Millipore). Protein integrity and oligomerization were checked on SDS–PAGE gels. Trimeric mRFPo (control) and mRFPovTSP1C (test) at 200 µg/ml in TBS containing either 2 mM $CaCl_2$ or 1 mM ethylene glycol tetraacetic acid were assayed for glycan binding on the Consortium for Functional Glycomics' glycan microarray (v3.2, 406 glycans; Smith *et al.*, 2010) by CFG Protein-Glycan Interaction Core H. Binding was analyzed directly by RFP fluorescence (excitation, 594 nm).

TSP1-binding assay

Rat-tail collagen I (1 µg/well; Sigma-Aldrich) or mRFPovTSP1C, mRFPovTSP1C/AAARE, or RFP control proteins (all at 30 nM) were coated in triplicate onto polystyrene 96-wells overnight at 4°C in TBS containing 2 mM $CaCl_2$. After blocking with 1% bovine serum albumin (BSA) in TBS containing 2 mM $CaCl_2$ and 0.1% Tween 20, 30 nM platelet TSP1 (Cell Sciences) was added for 1 h with rocking. Wells were washed three times with TBS containing 2 mM $CaCl_2$ and 0.01% Tween 20, incubated with goat N-20 antibody to TSP1 N-terminal domain for 1 h, washed again, incubated with rabbit anti-goat immunoglobulin G–horseradish peroxidase (Dako) for 1 h, washed again, and color developed with tetramethylbenzidine substrate (Pierce). We measured A_{450nm} in a Molecular Devices plate reader. The mean value from BSA-blocked wells was subtracted as background from the other results. Data were normalized on TSP1 binding to mRFPovTSP1C-coated wells. Three independent experiments were carried out.

Electron microscopy and analysis of collagen fibrils

C57Bl/6 *Thbs1*$^{-/-}$mice were originated as described (Lawler *et al.*, 1998) and were the gift of Jack Lawler. Tissue samples were obtained from wild-type or *Thbs1*$^{-/-}$ mice that had been killed in the laboratory of Takao Sakai at CCF. Mice were housed and killed according to CCF Institutional Review Board–approved procedures. For transmission electron microscopy, tail tendons or small (2 mm) squares of skin tissue were dissected from four 6.5- or 9-wk-old C57Bl/6 male or female wild-type or *Thbs1*$^{-/-}$ littermate mice, fixed for 3 h at 4°C in 1.5% glutaraldehyde and 1.5% paraformaldehyde in 0.1 M sodium cacodylate containing 0.05% $CaCl_2$ and 0.05% tannic acid (all from Electron Microscopy Science), and washed three times over 45 min at 4°C in 0.1 M sodium cacodylate or DMEM containing 0.05% $CaCl_2$. Tissues were rinsed in DMEM, postfixed in 1% OsO_4 in DMEM for 2 h, and then dehydrated and embedded in Spurr's epoxy. Ultrathin 70-nm sections were mounted onto Formvar-coated single-hole grids and observed using a FEI Tecnai G2 TEM operated at 120 kV. For samples from dermis, images were taken from matched planes of section in the upper, middle, and deep dermis from wild-type and *Thbs1*$^{-/-}$ samples. For all samples, areas of individual fibrils were measured from cross-sectional views in high power (52,900×) electron micrographs using ImageJ software. Eight fields were scored for each tissue sample from each mouse. All fibrils within each image were scored (430–700 fibrils/field in dermis and 200–350/field in tendon). Data were analyzed by frequency distribution and descriptive statistics.

Proliferation assay

Cell proliferation and viability were measured using CyQUANT Direct reagents (Invitrogen) according to the manufacturer's instructions.

Statistical analyses

Data are based on three independent experiments, unless otherwise stated. Statistical analyses were by unpaired Student's *t* test or one-way analysis of variance (ANOVA), with $p = 0.05$ taken as the threshold for significance.

ACKNOWLEDGMENTS

We thank the Protein-Glycan Interaction Core (Emory University School of Medicine, Atlanta, GA) of the Consortium for Functional Glycomics funded by National Institute of General Medical Sciences Grant GM62116 for analysis of samples on the glycan microarray; Kate Heesom for proteomic analysis; Takao Sakai and Keiko Sakai at the CCF for provision of mouse tissue; and the CCF Genomics core and MWG for DNA sequencing. This work was supported by National Institutes of Health Grants GM068073 and HL077107, British Heart Foundation studentship 09/038/2787 to E.D.C., and Medical Research Council Grant K018043.

REFERENCES

Adams JC (2001). Thrombospondins: multifunctional regulators of cell interactions. Annu Rev Cell Dev Biol 17, 25–51.

Adams JC, Bentley AA, Kvansakul M, Hatherley D, Hohenester E (2008). Extracellular matrix retention of thrombospondin 1 is controlled by its conserved C-terminal region. J Cell Sci 121, 784–795.

Adams JC, Lawler J (2011). The thrombospondins. Cold Spring Harb Perspect Biol 3, a009712.

Agah A, Kyriakides TR, Lawler J, Bornstein P (2002). The lack of thrombospondin-1 (TSP1) dictates the course of wound healing in double-TSP1/TSP2-null mice. Am J Pathol 161, 831–839.

Agarwal P, Zwolanek D, Keene DR, Schulz JN, Blumbach K, Heinegaard D, Zaucke F, Paulsson M, Kreig T, Koch M, Eckes B (2012). Collegen XII and XIV, new partners of cartilage oligomeric matrix protein in the skin extracellular matrix superstructure. J Biol Chem 287, 22549–24559.

Alford AI, Golicz AZ, Cathey AL, Reddy AB (2013). Thrombospondin-2 facilitates assembly of a type-I collagen-rich matrix in marrow stromal cells undergoing osteoblastic differentiation. Connect Tissue Res 54, 275–282.

Annis DS, Murphy-Ullrich JE, Mosher DF (2006). Function-blocking antithrombospondin-1 monoclonal antibodies. J Thromb Haemost 4, 459–468.

Bein K, Simons M (2000). Thrombospondin type 1 repeats interact with matrix metalloproteinase 2. Regulation of metalloproteinase activity. J Biol Chem 275, 32167–32173.

Bentley AA, Adams JC (2010). The evolution of thrombospondins and their ligand-binding activities. Mol Biol Evol 27, 2187–2197.

Bornstein P, Agah A, Kyriakides TR (2004). The role of thrombospondins 1 and 2 in the regulation of cell-matrix interactions, collagen fibril formation, and the response to injury. Int J Biochem Cell Biol 36, 1115–1125.

Burke A, Creighton W, Tavora F, Li L, Fowler D (2010). Decreased frequency of the 3'UTR T>G single nucleotide polymorphism of thrombospondin-2 gene in sudden death due to plaque erosion. Cardiovasc Pathol 19, e45–e49.

Calzada MJ, Kuznetsova SA, Sipes JM, Rodrigues RG, Cashel JA, Annis DS, Mosher DF, Roberts DD (2008). Calcium indirectly regulates immunochemical reactivity and functional activities of the N-domain of thrombospondin-1. Matrix Biol 27, 339–351.

Carlson CB, Bernstein DA, Annis DS, Misenheimer TM, Hannah BL, Mosher DF, Keck JL (2005). Structure of the calcium-rich signature domain of human thrombospondin-2. Nat Struct Mol Biol 12, 910–914.

Chanana B, Graf R, Koledachkina T, Pflanz R, Vorbruggen G (2007). AlphaPS2 integrin-mediated muscle attachment in Drosophila requires the ECM protein Thrombospondin. Mech Dev 124, 463–475.

Chen TL, Stevens JW, Cole WG, Hecht JT, Vertel BM (2004). Cell-type specific trafficking of expressed mutant COMP in a cell culture model for PSACH. Matrix Biol 23, 433–444.

Cockburn CG, Barnes MJ (1991). Characterization of thrombospondin binding to collagen (type I) fibres: role of collagen telopeptides. Matrix 11, 168–76.

Crawford SE, Stellmach V, Murphy-Ullrich JE, Ribeiro SM, Lawler J, Hynes RO, Boivin GP, Bouck N (1998). Thrombospondin-1 is a major activator of TGF-beta1 in vivo. Cell 93, 1159–1170.

DiCesare PE, Morgelin M, Mann K, Paulsson M (1994). Cartilage oligomeric matrix protein and thrombospondin 1. Purification from articular cartilage, electron microscopic structure, and chondrocyte binding. Eur J Biochem 223, 927–937.

Frolova EG, Drazba J, Krukovets I, Kostenko V, Blech L, Harry C, Vasanji A, Drumm C, Sul P, Jenniskens GJ, *et al.* (2014). Control of organization and function of muscle and tendon by thrombospondin-4. Matrix Biol 37, 35–48.

Frolova EG, Pluskota E, Krukovets I, Burke T, Drumm C, Smith JD, Blech L, Febbraio M, Bornstein P, Plow EF, *et al.* (2010). Thrombospondin-4 regulates vascular inflammation and atherogenesis. Circ Res 107, 1313–1325.

Gao AG, Lindberg FP, Finn MB, Blystone SD, Brown EJ, Frazier WA (1996). Integrin-associated protein is a receptor for the C-terminal domain of thrombospondin. J Biol Chem 271, 21–24.

Guex N, Peitsch MC (1997). SWISS-MODEL and the Swiss-PdbViewer: an environment for comparative protein modeling. Electrophoresis 18, 2714–2723.

Halasz K, Kassner A, Morgelin M, Heinegard D (2007). COMP acts as a catalyst in collagen fibrillogenesis. J Biol Chem 282, 31166–31173.

Hankenson KD, Sweetwyne MT, Shitaye H, Posey KL (2010). Thrombospondins and novel TSR-containing proteins, R-spondins, regulate bone formation and remodeling. Curr Osteoporos Rep 8, 68–76.

Holden P, Meadows RS, Chapman KL, Grant ME, Kadler KE, Briggs MD (2001). Cartilage oligomeric matrix protein interacts with type IX collagen, and disruptions to these interactions identify a pathogenetic mechanism in a bone dysplasia family. J Biol Chem 276, 6046–6055.

Isenberg JS, Martin-Manso G, Maxhimer JB, Roberts DD (2009). Regulation of nitric oxide signalling by thrombospondin 1: implications for anti-angiogenic therapies. Nat Rev Cancer 9, 182–194.

Isenberg JS, Ridnour LA, Dimitry J, Frazier WA, Wink DA, Roberts DD (2006). CD47 is necessary for inhibition of nitric oxide-stimulated vascular cell responses by thrombospondin-1. J Biol Chem 281, 26069–26080.

Jimenez B, Volpert OV, Crawford SE, Febbraio M, Silverstein RL, Bouck N (2000). Signals leading to apoptosis-dependent inhibition of neovascularization by thrombospondin-1. Nat Med 6, 41–48.

Kannus P, Jozsa L, Jarvinen TA, Jarvinen TL, Kvist M, Natri A, Jarvinen M (1998). Location and distribution of non-collagenous matrix proteins in musculoskeletal tissues of rat. Histochem J 30, 799–810.

Kvansakul M, Adams JC, Hohenester E (2004). Structure of a thrombospondin C-terminal fragment reveals a novel calcium core in the type 3 repeats. EMBO J 23, 1223–1233.

Kyriakides TR, Zhu YH, Smith LT, Bain SD, Yang Z, Lin MT, Danielson KG, Iozzo RV, LaMarca M, McKinney CE, *et al.* (1998). Mice that lack thrombospondin 2 display connective tissue abnormalities that are associated with disordered collagen fibrillogenesis, an increased vascular density, and a bleeding diathesis. J Cell Biol 140, 419–430.

Lawler J, Derick LH, Connolly JE, Chen JH, Chao FC (1985). The structure of human platelet thrombospondin. J Biol Chem 260, 3762–3772.

Lawler J, Sunday M, Thibert V, Duquette M, George EL, Rayburn H, Hynes RO (1998). Thrombospondin-1 is required for normal murine pulmonary homeostasis and its absence causes pneumonia. J Clin Invest 101, 982–992.

Merritt TM, Bick R, Poindexter BJ, Alcorn JL, Hecht JT (2007). Unique matrix structure in the rough endoplasmic reticulum cisternae of pseudoachondroplasia chondrocytes. Am J Pathol 170, 293–300.

Ozbek S, Balasubramanian PG, Chiquet-Ehrismann R, Tucker RP, Adams JC (2010). The evolution of extracellular matrix. Mol Biol Cell 21, 4300–4305.

Pablos JL, Everett ET, Leroy EC, Norris JS (1998). Thrombospondin 1 is expressed by mesenchymal cells in mouse post-natal skin and hair follicle development. Histochem J 30, 461–465.

Posey KL, Hankenson K, Veerisetty AC, Bornstein P, Lawler J, Hecht JT (2008). Skeletal abnormalities in mice lacking extracellular matrix proteins, thrombospondin-1, thrombospondin-3, thrombospondin-5, and type IX collagen. Am J Pathol 172, 1664–1674.

Posey KL, Hayes E, Haynes R, Hecht JT (2004). Role of TSP-5/COMP in pseudoachondroplasia. Int J Biochem Cell Biol 36, 1005–1012.

Posey KL, Hecht JT (2008). The role of cartilage oligomeric matrix protein (COMP) in skeletal disease. Curr Drug Targets 9, 869–877.

Sabatier L, Chen D, Fagotto-Kaufmann C, Hubmacher D, McKee MD, Annis DS, Mosher DF, Reinhardt DP (2009). Mol Biol Cell 20, 846–858.

Satoh T, Cowieson NP, Hakamata W, Ideo H, Fukushima K, Kurihara M, Kato R, Yamashita K, Wakatsuki S (2007). Structural basis for recognition of high mannose type glycoproteins by mammalian transport lectin VIP36. J Biol Chem 282, 28246–28255.

Schultz-Cherry S, Chen H, Mosher DF, Misenheimer TM, Krutzsch HC, Roberts DD, Murphy-Ullrich JE (1995). Regulation of transforming growth factor-beta activation by discrete sequences of thrombospondin 1. J Biol Chem 270, 7304–7310.

Smith DF, Song X, Cummings RD (2010). Use of glycan microarrays to explore specificity of glycan-binding proteins. Methods Enzymol 480, 417–444.

Sodersten F, Ekman S, Eloranta ML, Heinegard D, Dudhia J, Hultenby K (2005). Ultrastructural immunolocalization of cartilage oligomeric matrix protein (COMP) in relation to collagen fibrils in the equine tendon. Matrix Biol 24, 376–385.

Stenina OI, Desai SY, Krukovets I, Kight K, Janigro D, Topol EJ, Plow EF (2003). Thrombospondin-4 and its variants: expression and differential effects on endothelial cells. Circulation 108, 1514–1519.

Stenina OI, Topol EJ, Plow EF (2007). Thrombospondins, their polymorphisms, and cardiovascular disease. Arterioscler Thromb Vasc Biol 27, 1886–1894.

Subramanian A, Wayburn B, Bunch T, Volk T (2007). Thrombospondin-mediated adhesion is essential for the formation of the myotendinous junction in Drosophila. Development 134, 1269–1278.

Tan K, Duquette M, Joachimiak A, Lawler J (2009). The crystal structure of the signature domain of cartilage oligomeric matrix protein: implications for collagen, glycosaminoglycan and integrin binding. FASEB J 23, 2490–2501.

Tan K, Duquette M, Liu JH, Zhang R, Joachimiak A, Wang JH, Lawler J (2006). The structures of the thrombospondin-1 N-terminal domain and its complex with a synthetic pentameric heparin. Structure 14, 33–42.

Topol EJ, McCarthy J, Gabriel S, Moliterno DJ, Rogers WJ, Newby LK, Freedman M, Metivier J, Cannata R, O'Donnell CJ, *et al.* (2001). Single nucleotide polymorphisms in multiple novel thrombospondin genes may be associated with familial premature myocardial infarction. Circulation 104, 2641–2644.

Yang Z, Kyriakides TR, Bornstein P (2000). Matricellular proteins as modulators of cell-matrix interactions: adhesive defect in thrombospondin 2-null fibroblasts is a consequence of increased levels of matrix metalloproteinase-2. Mol Biol Cell 11, 3353–3364.

Yee KO, Connolly CM, Duquette M, Kazerounian S, Washington R, Lawler J (2009). The effect of thrombospondin-1 on breast cancer metastasis. Breast Cancer Res Treat 114, 85–96.

Zhang X, Lawler J (2007). Thrombospondin-based antiangiogenic therapy. Microvasc Res 74, 90–99.